54th International Astronautical Congress of the International Astronautical Federation, the International Academy of Astronautics and the International Institute of Space Law
29 September - 3 October 2003, Bremen, Germany

IAC-03-A.P.08

PRELIMINARY ANALYSIS OF INTERPLANETARY TRAJECTORIES WITH AEROGRAVITY AND GRAVITY ASSIST MANOEUVRES

Stefano M. Pessina
Politecnico di Milano University
Milan, Italy
stepex@tin.it

Stefano Campagnola
ESA/ESOC - Mission Analysis Office
Darmstadt, Germany
Stefano.Campagnola@esa.int

Massimiliano Vasile
ESA/ESTEC - Advanced Concepts Team
Noordwijk, The Netherlands
Massimiliano.Vasile@esa.int

ABSTRACT

In this paper a preliminary analysis of a wide range of mission opportunities, offered by either aerogravity assist or gravity assist manoeuvres, has been carried out. After an accurate validation of aerogravity assist traditional analytical models, according to several different criteria an extensive global search for optimal trajectories has been performed for high-energy missions, resorting to gravity and aerogravity manoeuvres. To this aim, the new preliminary analysis tool PAMSIT, based on some simplified hypotheses, has been developed. This is capable of efficiently and exhaustively exploring the solutions space for this particular problem, considering the feasibility of a trajectory from both the orbital energy and phasing points of view. Then, all found solutions have been classified according to launch and arrival velocities, time of flight and planetary encounters. A comparison between the opportunities offered by gravity manoeuvres and aerogravity manoeuvres will be presented showing the advantages of the latter in all analysed cases. In particular some interesting options for missions to Jupiter and Neptune will be presented.

INTRODUCTION

The use of the gravitational field of a celestial body to obtain a suitable change in spacecraft's velocity modulus and direction has proved to be a very efficient strategy when high levels of ΔV are required. Some space missions, otherwise unfeasible due to the current performances of launchers and propulsion systems, made successfully use of gravity assist manoeuvres (GA) to put the spacecraft in high inclined or high energetic orbits.

More recent analyses on aerogravity assist (AGA) have demonstrated how this type of manoeuvres could be an interesting alternative to simple GA. In fact, while performing a flyby at a planet, it is possible to exploit not only its gravity attraction but also its atmosphere, providing the spacecraft with appropriate lifting surfaces. Shapes with a high aerodynamic efficiency can reduce the loss in velocity due to drag; therefore, under these conditions, the ΔVs obtainable can be significantly higher then the ones provided by gravity-only manoeuvres.

Several authors have analysed the problem, in particular McRonald and Randolph[1,2,3] proposed aerogravity assist at Venus (V_{AGA}), at Earth (E_{AGA}), at Mars (M_{AGA}) and the AGA sequence Venus-Mars (V_{AGA}-M_{AGA}) for high demanding interplanetary missions, such as a solar probe or a mission to Pluto. With reference to the same targets, Lohar, Misra and Mateescu[4] analysed the use of a Jupiter gravity assist (J_{GA}) in combination with M_{AGA} and V_{AGA}-M_{AGA}, and also the sequence of manoeuvres V_{GA}-M_{AGA}-J_{GA}. Efficient ways of designing trajectories involving GA have been implemented in tools like STOUR[5,6], by

Petropoulos, Longuski, and Bonfiglio[7] who made an accurate search of multiple GA trajectories to Jupiter. In particular, Bonfiglio[8] derived analytical models of the AGA manoeuvre, performing a preliminary numerical comparison of various methods. He also introduced an AGA-trajectories search method, combining it with STOUR, and he analysed different flyby sequences for missions to Neptune and to Pluto and also for Mars, Venus and Saturn free-return missions. These considerations were furthermore developed by Bonfiglio, Longuski and Vinh[9]. Strange and Longuski[10] proposed a graphical method, based on Tisserand Graphs for GA trajectory analysis, without phasing considerations. Then Johnson and Longuski[11], considering missions with AGA, also adopted this graphical technique. Finally, McRonald, Randolph, Lewis, Bonfiglio, Longuski and Kolodziej[12], with reference to AGA-missions, presented results regarding vehicle configuration designs, parametric trajectory studies, materials research and atmospheric flight simulations.

In this paper the effectiveness of the AGA manoeuvres with respect to the GA ones is investigated, giving an exhaustive comparison between the two strategies throughout an analysis of a wide range of possible flyby sequences. To this aim, a new tool, called PAMSIT (Preliminary Analysis of Multiple Swingbys Interplanetary Trajectories), has been developed. In the recent times, global optimisation tools[6,8,10,11,13,14,15,16,17,18,19] have been investigated, making use of either stochastic or deterministic approaches (or a combination of both), in order to help mission analysts in designing interplanetary trajectories. PAMSIT is a MATLAB® software tool for preliminary analysis and design of multiple AGA-GA trajectories for space missions in the Solar System, such as planetary exploration, Sun observation and free-return missions. On the basis of some simplified hypotheses, the code analyses a variety of multiple swingbys trajectories with gravity and/or aerogravity assist manoeuvres, using an automated search method. As it will be demonstrated, the good quality of the solutions generated by the simplified model implemented in PAMSIT makes them interesting both for preliminary mission design and as initial guesses for more detailed analysis.

Prior to the comparison between AGA and GA, the errors introduced by the present AGA analytical models are studied, considering also the consequence of aerodynamic drag acting on the spacecraft in the hyperbolic incoming and outgoing transition arcs of the AGA manoeuvre.

GA AND AGA MODELS

Gravity assist manoeuvres are here modelled with a linked-conic approximation. If the hyperbolic motion during a flyby is not perturbed and no ΔV-manoeuvres are performed, the modulus of the incoming relative velocity v_∞^- is equal to the modulus of the outgoing one v_∞^+ (see Figure 1, where V_{Planet} is the planet velocity in the heliocentric reference frame). We call e and r_P respectively the eccentricity and the periapsis radius of the relative trajectory, while μ is the gravitational parameter of the central body; then, the total deviation angle ϕ (see Figure 1 and Figure 2) can be found as follows:

$$\phi = 2\arcsin(1/e)\,,\; e = 1 + r_P\,(v_\infty^-)^2/\mu \qquad (1)$$

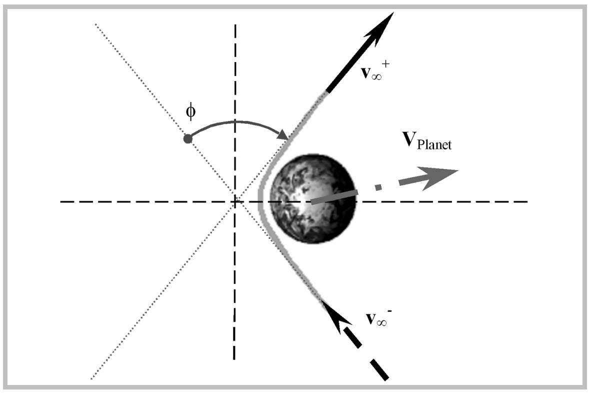

Figure 1: Generic GA relative trajectory

The GA vector diagram is shown in Figure 2, indicating with $\mathbf{V}^-$ and $\mathbf{V}^+$ the incoming and outgoing spacecraft absolute velocity (heliocentric reference frame), with $\Delta\mathbf{V}$ the variation in velocity and with α^- and α^+ the angle between v_∞ and V_{Planet}, respectively before and after the flyby.

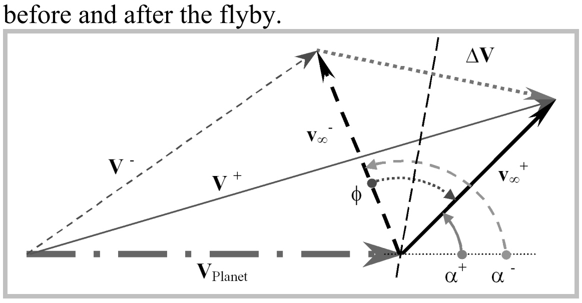

Figure 2: GA vector diagram

AGAs are modelled as in literature[2,3,8,9,12,20] (see Figure 3). The main idea is that a lifting body performs a flight through the atmosphere of a suitable planet; exploiting the aerodynamic forces, it augments the total deviation angle ϕ, with respect to a manoeuvre assisted only by gravity. The spacecraft approaches the planet along a path, which is a hyperbola in the planet-centred reference frame. Preserving a zero-lift attitude, it reaches the periapsis. Then, it flies at a constant altitude, controlling its attitude as the velocity changes, in order to balance the centrifugal force with the gravitational attraction and the aerodynamic lift (pointing towards the surface). The balance of forces that allows the constant altitude flight is:

$$\rho v^2 S C_L / 2 + m\mu / r^2 = m v^2 / r \quad (2)$$

where ρ is the atmospheric density, v is the spacecraft relative velocity (planet-centred reference frame), S is the reference area for aerodynamic coefficient definition of the vehicle, C_L is the lift coefficient, m is the spacecraft mass and r is the distance from spacecraft to central body.

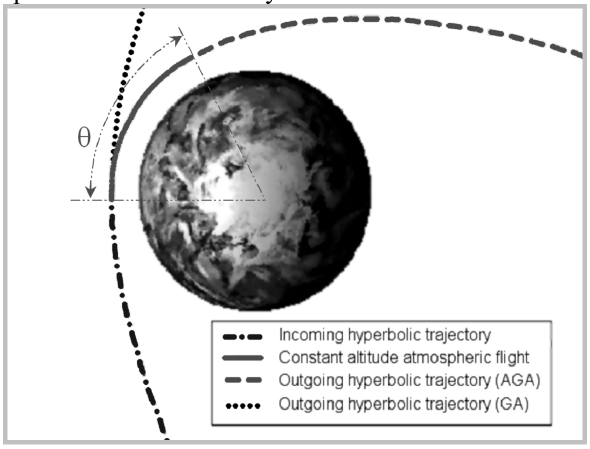

Figure 3: Generic AGA relative trajectory

When the desired atmospheric turn angle (θ, see Figure 3) is reached, with a breakaway manoeuvre the spacecraft reverses its lift (or simply sets it to zero), thus starting a hyperbolic exit trajectory. Note that aerodynamic drag acts on the probe during the whole AGA trajectory. As a consequence, the v_∞^+ is no longer the same as v_∞^-, the spacecraft being braked along its path.

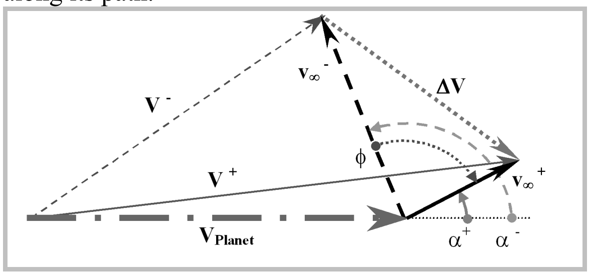

Figure 4: AGA vector diagram

The main advantage in performing an AGA is the higher deviation angle ϕ that can be obtained. The loss in velocity due to drag can be minimized by hypersonic vehicles with high maximum aerodynamic efficiency E^*, such as waveriders. The energy loss being limited, it is possible to take full advantage of the increased angular deflection, obtaining a bigger ΔV (e.g. in Figure 2 and Figure 4). Aerogravity assists are possible whenever the planet presents an appropriate atmosphere. In this work, Venus, Earth and Mars have been considered as suitable candidates and their atmospheres have been modelled on the basis of data found in literature[21,22,23].

The incoming and outgoing arcs of the AGA relative trajectory can be modelled supposing they are unperturbed hyperbolas.

To model the constant altitude phase, it is assumed a general drag polar equation for the waverider:

$$C_D = C_{D0} + k \left| C_L \right|^n \quad (3)$$

where C_{D0} is the zero-lift drag coefficient, k is the correction factor and n is the polar exponent.

Assuming a bi-dimensional motion, the atmospheric turn angle θ can be expressed as a function of a dimensionless speed variable u and dimensionless glide-altitude parameter η[8,9] according to the following differential equation:

$$d\theta = -\frac{1}{2} E^* \frac{n \eta^{n-1} u^{n-1}}{(n-1)\eta^n u^n + (u-1)^n} du \quad (4)$$

$$\text{where:} \quad u = r \cdot v^2 / \mu; \;\; \eta = 0.5 \rho r S C_L^* / m \quad (5)$$

Three analytical solutions of (4) are available[8,9], providing the atmospheric turn angle θ as a function of the spacecraft velocity at periapsis of the incoming and outgoing trajectory (v_P^- and v_P^+); these correspond to the values n=1, n=2 and n=1.5 in (3).

The solution with n=1 can be arranged[8,9,20] to solve v_P^+ as a function of v_P^- and θ:

$$v_P^+ = \sqrt{[(v_P^-)^2 - \mu / r] \cdot e^{-2\theta/E^*} + \mu / r} \quad (6)$$

Otherwise, numerical solvers are needed to obtain v_P^+ from v_P^- and θ with n=2 and n=1.5.

NUMERICAL COMPARISON OF AGA MODELS

Since the current model for the waverider[24] uses n=1.75 in (3), a numerical comparison of the AGA models have been carried out in order to find which one of the value of n is the most suitable to model the AGA manoeuvre.

Coefficients in (3) are taken from experimental data on a hypersonic waverider[24], having chosen the planform area as reference surface S .

Chosen the aerodynamic shape, dimensions are fixed supposing that the spacecraft has to fit the STS cargo bay (4.57 m diameter by 18.3 m length). A mass of 1000 kg has been taken as nominal. Features of selected AGA vehicle are summarized in Table 1.

Geometry		Aerodynamics	
Length	11 m	C_{D0}	0.00828
Span	4.57 m	k	1.1
Base height	1.93 m	n	1.75
Planform area	29.843 m^2	E*	3.7328
Base area	5.141 m^2	C_L*	0.0721
Volume	16.164 m^3	Mass	1000 kg

Table 1: Features of selected AGA vehicle

Ignoring perturbations, ΔV-manoeuvres and drag losses approaching the planet, the spacecraft velocity at periapsis of the incoming trajectory (v_P^-) is:

$$v_P^- = \sqrt{(v_\infty^-)^2 + 2\mu / r_P} \qquad (7)$$

In order to reduce the drag effects, we assume to reach the maximum aerodynamic efficiency E^* at the beginning of the atmospheric flight.
According to (2) and (7), this brings to:

$$\frac{1}{2}\rho(r) C_L^* \frac{S}{m}[r_P (v_\infty^-)^2 + 2\mu] - \frac{\mu}{r_P} - (v_\infty^-)^2 = 0 \qquad (8)$$

where C_L^* is the lift coefficient at maximum aerodynamic efficiency.
From (8), for each planetary atmosphere model it is then possible to evaluate the altitude z that verifies this condition as a function of the incoming relative velocity v_∞^-. Results regarding selected waverider are shown in Figure 5.

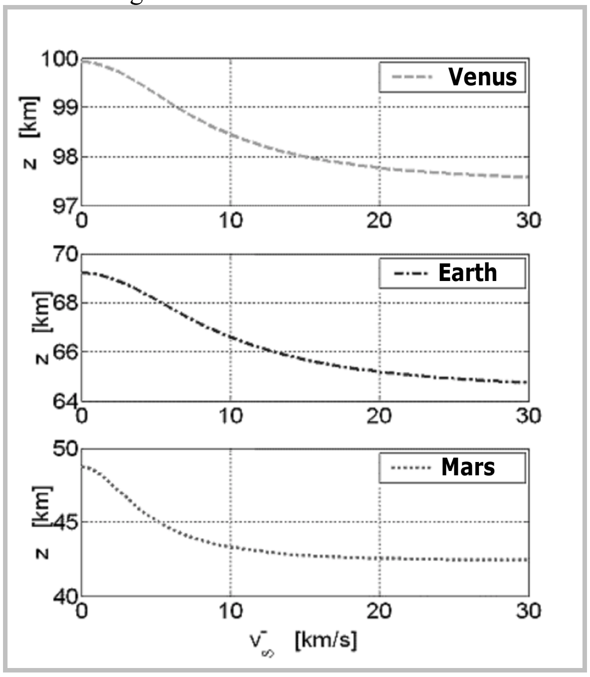

Figure 5: Altitudes that allow the selected waverider to start the constant altitude flight at E^*

The comparison among AGA models has been done on the basis of the following assumptions:

- Venus, Earth and Mars are used as AGA bodies.
- Periapsis radii of the incoming trajectory are those shown in Figure 5.
- Waverider characteristics are taken from Table 1.
- Only trajectories with total turning angle ϕ less than 180° and with both incoming and outgoing hyperbolic arcs are considered.

The incoming relative velocity (v_∞^-) is varied from 0 to 30 km/s and the atmospheric turn angle (θ) from 0° to 180°. The total deviation angle (ϕ) and the outgoing hyperbolic trajectory at infinity (v_∞^+) are calculated for each combination of discretised parameters.
The following analyses have been performed:

- Case 1: We compute three sets of solutions corresponding to the three models of the entire AGA-manoeuvre. Each of them is composed of a keplerian incoming hyperbola, the analytical model for the constant altitude flight (with n=1, n=2 or n=1.5) and a keplerian outgoing hyperbola. A numerical solver is used when n=2 and n=1.5, while for n=1 we use (6).
- Case 2: We calculate the solutions for a model with unperturbed incoming and outgoing arcs, solving the dynamic in the atmospheric phase by numerical integration of (4) with n=1.75.
- Case 3: Assuming a zero-lift attitude (C_L=0 and C_D= C_{D0}) during the incoming and outgoing arcs and using in the constant altitude phase (4) with n=1.75, we run numerical integrations of the dynamics of the entire trajectories.

Each set of solutions derived in Case 1 is then compared with solutions of Case 2 and 3.
From the comparison between Case 1 and 2, it is possible to evaluate the inaccuracy due to the use of an approximated solution, based on a value of n different from the real one. Comparing Case 1 and 3, we estimate the global errors of the three complete AGA models.
We define the percentage errors $\tilde{E}$ of the quantity z (where z is the total deviation angle ϕ or the outgoing velocity at infinity v_∞^+) to perform a comparison between Case x and Case y, as follows:

$$\tilde{E}_z^{(x,y)} = \frac{z^{(x)} - z^{(y)}}{z^{(y)}} \cdot 100 \qquad (9)$$

Obtained results are shown in Table 2 and in Table 3.

		n=1	n=1.5	n=2
Mean $\tilde{E}_\phi^{(1,2)}$	*Venus*	0.044	0.015	-0.014
	Earth	0.049	0.016	-0.015
	Mars	0.018	0.006	-0.005
Mean $\tilde{E}_{v_\infty^+}^{(1,2)}$	*Venus*	-0.253	-0.086	0.089
	Earth	-0.275	-0.093	0.092
	Mars	-0.115	-0.043	0.029

Table 2: Comparison between Case 1 and Case 2

		n=1	n=1.5	n=2
Mean $\tilde{E}_\phi^{(1,3)}$	*Venus*	0.488	0.460	0.433
	Earth	0.689	0.659	0.628
	Mars	0.465	0.454	0.444
Mean $\tilde{E}_{v_\infty^+}^{(1,3)}$	*Venus*	-2.115	-1.979	-1.847
	Earth	-2.847	-2.705	-2.566
	Mars	-2.489	-2.435	-2.382

Table 3: Comparison between Case 1 and Case 3

It can be seen from Table 2 that errors due to the use of the analytical models, based on values of n different from the real one, are small in all cases. The drag effect in the incoming and outgoing legs could be significant, although a zero-lift attitude has been assumed. In fact (see Table 3) greater errors have been obtained on v_∞^+, due to the assumption of lack of perturbation in the entry and exit trajectories.

Furthermore, in the second run critical errors have been obtained for low v_∞^- and great θ, due to excessive loss in velocity in the incoming and outgoing arcs. Using one of the AGA models for an automated search method of optimal trajectories, it's necessary to verify the feasibility of results by numerical integration if they involve one of the above-mentioned critical situations. One example of the trend of the percentage error on v_∞^+ is shown in Figure 6, having analysed typical AGA incoming velocities (10 km/s < v_∞^- < 15 km/s).

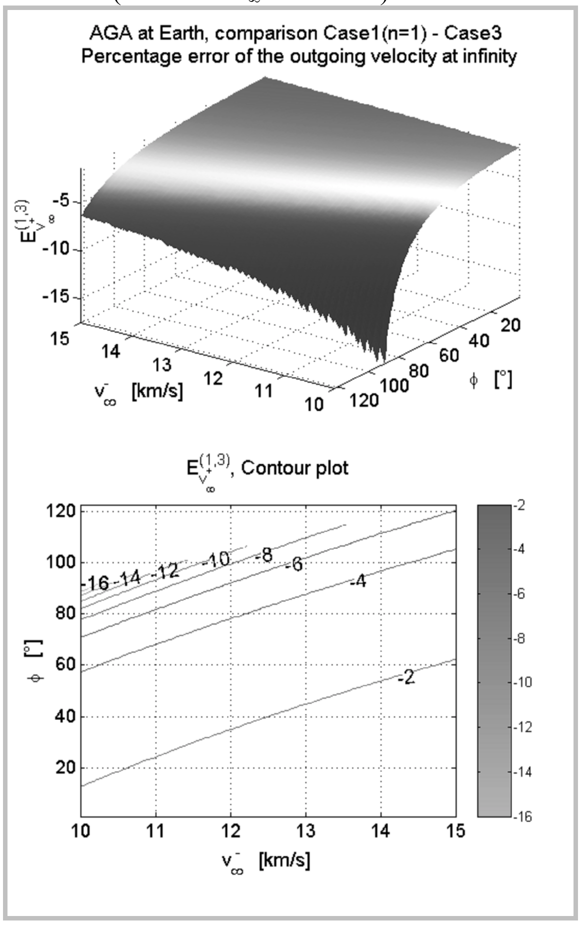

Figure 6: Example of the trend of % error on v_∞^+

As a general result, the best approximation is provided by the n=2 case. Nevertheless, the approximations due to different n appear negligible and the errors remain low, so that n=1 has been chosen for sake of simplicity, since in this case the straightforward explicit equation (6) can be used.

PAMSIT

In order to search for all possible trajectories with either AGA or GA manoeuvres, the two models presented above have been implemented in a software tool specifically developed for preliminary design of multiple swingby trajectories.

This new tool, called PAMSIT (Preliminary Analysis of Multiple Swingbys Interplanetary Trajectories), investigates all possible trajectories to a specified target and selects the ones that minimise a predefined merit function.

PAMSIT uses a simplified model of the Solar System with circular coplanar orbits of the planets; assuming the spacecraft motion to be in the same plane of the planets, it looks for quasi-ballistic solutions, systematically spanning all the solution space.

PAMSIT performs two different analyses:

A. Energy-based feasibility study
B. Phasing (timing) feasibility study

In the A-type study, given a specific target, all possible permutations of intermediate planetary flybys (GA or AGA) are analysed, ignoring the phasing problem. Only trajectories that remain hyperbolic (relative to the planet) for the whole flybys are considered.

Launch excess velocity as well as GA and AGA parameters are discretised. In case of GA, the periapsis radii of the relative hyperbolas are discretised, disregarding periapsis altitudes that don't guarantee a safe passage. The limit-altitudes are 200 km at the terrestrial planets and Pluto, 5 Jovian radii at Jupiter (in order to migrate radiation), 2 planetary radii at Saturn and one planetary radius at Uranus and Neptune (to avoid rings). Whenever performing an AGA, the periapsis radius of the incoming relative trajectory is chosen according to Figure 5, while the atmospheric turn angle θ is discretised; the maximum value is the one that causes a parabolic outgoing trajectory, if the total deviation ϕ remains lower then 180°. While executing a flyby, both positive and negative deviation angles ϕ are considered, respectively augmenting or lowering the angle α^+ with respect to α^- (see Figure 2 and Figure 4, where the α-lowering case is shown).

Once determined the orbital parameters of one phase between two consecutive planetary encounters, all the possible transfers are investigated and the different times of flight are calculated[10] (see Figure 7). In case of consecutive encounters with the same planet, also resonant transfers are considered.

For each different interplanetary path, among all feasible trajectories, the one with the lowest time of flight (ToF) is saved. Despite the lacking of the phasing problem, A-type provides the user with a lower bound for the ToF. Furthermore, it finds which strategies are feasible using only energy-based considerations, thus reducing the computational time of the subsequent analysis, which introduces the phasing model, inasmuch as unfeasible solutions can be now disregarded.

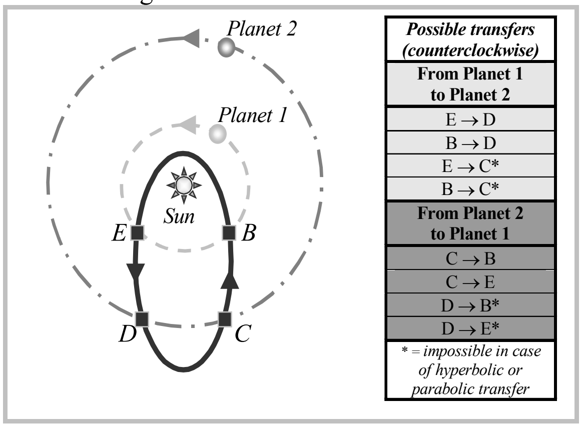

Figure 7: Different transfers on the same orbit

In the B-type study the basic structure of the algorithm is preserved, but some modifications are introduced, in order to consider the phasing problem. An improved model of the Solar System is used, including the mean motion of the planets in circular and coplanar orbits. By varying the launch date, the position of the spacecraft at the rendezvous dates is constrained to match the position of the swingby planets, within predefined tolerances. A finite number of bound orbits can be performed before each planetary encounter. Sets of interesting solutions can be selected, choosing suitable merit functions made by a combination of the following:

- ToF , i.e. the time of flight of the entire mission.
- ΔV_L , i.e. the escape ΔV kick from an elliptical to a hyperbolic coplanar trajectory, performed at the periapsis.
- ΔV_A , i.e. the capture ΔV from a hyperbolic to an elliptic coplanar orbit, always in the periapsis.

The general form of the measure of merit (MM) we have adopted is defined as follows:

$$MM = w_1 \cdot ToF + w_2 \cdot \Delta V_L + w_3 \cdot \Delta V_A ; \qquad (10)$$

We consider as initial conditions a circular orbit around the Earth at 200 km altitude. The target is a bound orbit around the final planet, with a periapsis altitude equal to the limit flyby-altitude for a safe passage (previously mentioned) and an apoapsis radius of 250 planetary radii. In (10) we use as a unit of measurement km/s for ΔVs and sidereal years for ToF, while the choice of the weight coefficients w_i is mission dependant. Automated trade-offs can be made among all feasible solutions found, looking for those minimising the selected MMs. These can be used for preliminary mission analysis studies, but also as initial guesses for local optimisation tools, in order to restore the feasibility in a more complete model, using very limited ΔVs.

The following is the glossary of the abbreviations used in labelling interplanetary paths for the solutions that will be shown: Y = Mercury, V = Venus, E = Earth, M = Mars, J = Jupiter, S = Saturn, U = Uranus, N = Neptune, P = Pluto. X_{GA} and X_{AGA} indicate respectively a GA or AGA flyby at planet X, while X_L and X_A launch from and arrival at planet X.

Verification of PAMSIT

The accuracy of the solutions obtained with PAMSIT has been assessed optimising some of them with DITAN[14], a software developed under ESA contract for the design of gravity assist low-thrust trajectories. The whole trajectory is divided into phases, starting from launch or from a planetary manoeuvre, ending with the following planetary encounter. A discontinuity in the velocity vector is introduced in between each phase, thus modelling an impulsive manoeuvre. The total ΔV is then minimised, while the departure relative velocity ($v_{\infty,L}$) is fixed and the arrival relative velocity ($v_{\infty,A}$) is allowed to vary.

The optimised solutions resulted to be very close to the correspondent first guesses obtained by PAMSIT in terms of planetary encounters dates. Furthermore, the total ΔV costs necessary to restore feasibility remained low (in all tested cases, below 300 m/s). Therefore, the physical model seems to be consistent and the assumed tolerance at planetary rendezvous conservative. The latter could be increased augmenting the number of launch possibilities, the feasibility of new solutions should be verified and higher corrective-ΔVs are expected.

As an example, a comparison between a first guess solution and a correspondent optimised trajectory is presented in Table 4.

	First Guess		**Optimised**	
	Date	ΔV [km/s]	Date	ΔV [km/s]
Launch from Earth	24/7/2010	4	17/8/2010	4
Manoeuvre 1	18/9/2010	---	6/9/2010	0
GA 1: Venus	13/11/2010	2.823	11/11/2010	3.115
Manoeuvre 2	14/4/2011	---	1/5/2011	0
GA 2: Earth	14/9/2011	5.779	17/9/2011	6.665
Manoeuvre 3	13/9/2012	---	7/9/2012	0
GA 3: Earth	13/9/2013	6.976	17/9/2013	7.351
Manoeuvre 4	23/6/2015	---	29/6/2014	0.077
Arrival to Jupiter	31/3/2017	6.385	25/12/2016	5.55

Table 4: Comparison between a first guess solution, and correspondent optimised trajectory

This refers to a mission to Jupiter with launch in 2010, making use the gravity assist sequence Venus-Earth-Earth (see Figure 8 and Figure 9).

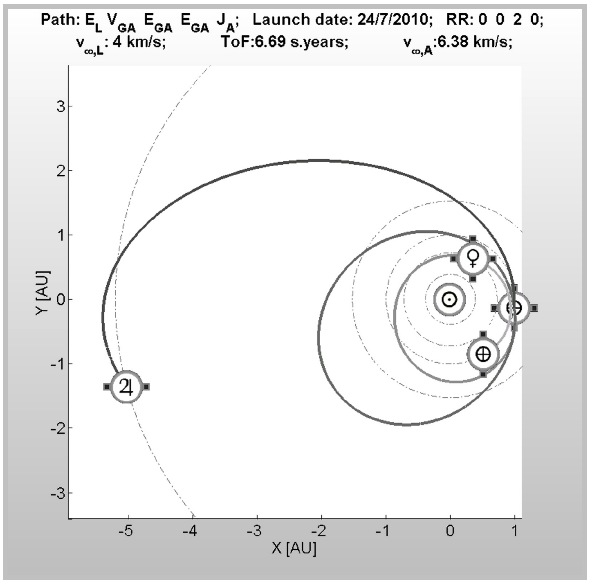

Figure 8:First guess solution, provided by PAMSIT

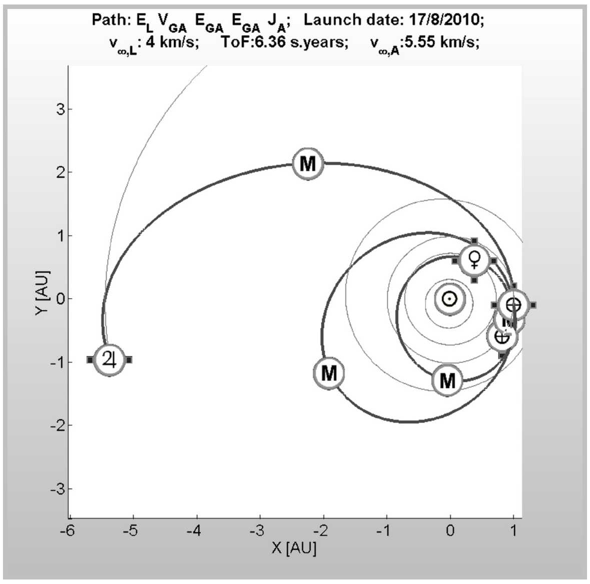

Figure 9:Optimised trajectory, performed by DITAN

COMPARISON BETWEEN AGA AND GA STRATEGIES

In order to compare the performances achievable using only gravity assist and using aerogravity assist (in combination with or in substitution to GA), a preliminary purely energetic analysis will be performed. Therefore, the actual position of the planets is not taken into account and we look for the maximum performances theoretically achievable in both cases, only on the basis of energetic considerations.

Then, a second analysis will follow taking into account the actual phase of the planets and in particular two missions of great scientific interest, to Jupiter and to Neptune, will be studied and we will show optimal launch options in the two cases, according to different figures of merit.

Energy-based analysis: high energy missions

The energy-based feasibility study above mentioned is now applied to investigate some of the most demanding missions for the Solar System exploration, such as missions to outer planets and a mission for Sun observation.

For missions to planets, the final target is the sphere of influence of the selected celestial body, while for the Sun observation mission the final target is a perihelion distance of four solar radii.

Three possible escape velocities ($v_{\infty,L}$) from Earth are considered: 3 km/s, 5 km/s and 7 km/s. For resonant orbit, the ratio RR=N/D is changed varying both N and D from 1 to 4. The maximum g-load bearable by the spacecraft during flybys is set equal to 12, while no limit on ToF is introduced. Paths involving only gravity assist manoeuvres (called GA-only) are compared to strategies that consider also aerogravity assist manoeuvres in combination with or in substitution to GA (called AGA+GA).

	GA-only (without considering phasing)		
	$v_{\infty,L}$ = 3 km/s	$v_{\infty,L}$ = 5 km/s	$v_{\infty,L}$ = 7 km/s
to Jupiter	V_{GA} E_{GA} V_{GA} E_{GA} 2.663 years	V_{GA} V_{GA} E_{GA} M_{GA} 1.466 years	V_{GA} V_{GA} E_{GA} M_{GA} 1.371 years
to Saturn	V_{GA} E_{GA} E_{GA} J_{GA} 6.204 years	V_{GA} V_{GA} M_{GA} J_{GA} 3.732 years	V_{GA} E_{GA} M_{GA} J_{GA} 3.345 years
to Uranus	V_{GA} E_{GA} E_{GA} J_{GA} 9.664 years	V_{GA} V_{GA} E_{GA} J_{GA} 6.413 years	V_{GA} E_{GA} M_{GA} J_{GA} 6.190 years
to Neptune	V_{GA} E_{GA} E_{GA} J_{GA} 13.009 years	V_{GA} V_{GA} E_{GA} J_{GA} 9.063 years	V_{GA} V_{GA} E_{GA} J_{GA} 8.858 years
to Pluto	V_{GA} E_{GA} E_{GA} J_{GA} 15.938 years	V_{GA} V_{GA} E_{GA} J_{GA} 11.381 years	V_{GA} V_{GA} E_{GA} J_{GA} 11.135 years
to Sun	--- ---	V_{GA} V_{GA} E_{GA} J_{GA} 4.804 years	V_{GA} V_{GA} E_{GA} J_{GA} 4.781 years

Table 5: GA-only strategies that allow minimum ToF

	AGA+GA (without considering phasing)		
	$v_{\infty,L}$ = 3 km/s	$v_{\infty,L}$ = 5 km/s	$v_{\infty,L}$ = 7 km/s
to Jupiter	V_{GA} E_{AGA} M_{AGA} 1.798 years	V_{AGA} E_{AGA} M_{AGA} 1.342 years	V_{AGA} V_{GA} E_{AGA} 1.203 years
to Saturn	V_{GA} E_{AGA} M_{AGA} 3.250 years	V_{AGA} E_{AGA} M_{AGA} 2.297 years	V_{AGA} V_{GA} E_{AGA} 2.164 years
to Uranus	V_{GA} E_{AGA} M_{AGA} 7.395 years	V_{AGA} E_{AGA} M_{AGA} 4.555 years	M_{AGA} V_{AGA} E_{AGA} 3.952 years
to Neptune	V_{GA} E_{AGA} M_{AGA} 13.197 years	V_{AGA} E_{AGA} M_{AGA} 7.242 years	M_{AGA} V_{AGA} E_{AGA} 5.950 years
to Pluto	V_{GA} E_{AGA} M_{AGA} 18.961 years	V_{AGA} E_{AGA} M_{AGA} 9.630 years	M_{AGA} V_{AGA} E_{AGA} 7.705 years
to Sun	--- ---	V_{GA} E_{AGA} J_{GA} 3.375 years	V_{AGA} E_{AGA} J_{GA} 3.245 years

Table 6: AGA+ strategies that allow minimum ToF

For the AGA+GA case, we assume that E^* is equal to 3.73 (see Table 1). Since AGA presents in general better performances than GA, a maximum of 4 intermediate encounters with planets are considered for GA, while a maximum of 3 planetary manoeuvres are allowed in case of AGA+GA.

The results (listed in Table 5 and Table 6) are comparable with those presented in previous papers and obtained with a different method, based on the discretisation of Tisserand Graphs[10,11].

As it can be seen, AGA allows faster trajectories than GA even with fewer flybys. This is true for all the targets and $v_{\infty,L}$ with two exceptions: missions to Neptune and Pluto with $v_{\infty,L} = 3$ km/s. In these cases, due to low launch velocity and high energy required to reach final targets, the reduced number of flyby is too penalizing. For missions to planets beyond Jupiter, a Jovian flyby is always required for GA-only options, thus significantly limiting the launch windows because of the dependence on Jupiter phasing, while AGA+GA fastest trajectories only requires gravity or aerogravity swingbys of inner planets. Due to high-energy requirements, no feasible trajectories are found for missions to the Sun at the lowest value of $v_{\infty,L}$, both considering the GA-only and the AGA+GA strategies.

<u>Phasing feasibility study: Missions to Jupiter</u>

A more detailed analysis with phasing considerations is now performed for missions to Jupiter. It is a target of great scientific interest and a mission to the Jovian moon Europa has been considered in recent times, in order to prove the existence of exobiology.

We consider a time period of 5 years, from the 1st of January 2007 to the 1st of January 2012, with a discretisation step of 1 Julian day, and we vary the $v_{\infty,L}$ from 2.5 km/s to 7 km/s, with a discretisation step of 0.25 km/s. Defining RR=N/D as resonant ratio, we vary both N and D from 1 to 4, while the maximum allowable number of multiple bound orbits before each planetary encounter is set to 4. The maximum g-load bearable by the spacecraft during flybys is 12 and the maximum allowable ToF is set equal to 7 sidereal years. The tolerance between the angular position of the spacecraft and of planets at the rendezvous dates is set equal to 5°. For the AGA+GA case, we assume that E^* is equal to 3.73 (see Table 1). The A-type analysis found a set of possible paths that are further investigated by the B-type analysis. We analyse 13 different flyby sequences for GA-only and 18 for AGA+GA. It can be noticed that some of the paths apparently feasible in the energy-based analysis are in fact unfeasible if the actual motion of the planets is considered (4 for GA-only and 2 for AGA+GA).

According to (10) and fixing different weights ($\mathbf{w}=[w_1, w_2, w_3]$), we use three measures of merit:

- MM1: low $v_{\infty,L}$ and $v_{\infty,A}$, short ToF; $\mathbf{w}=[0.75, 1, 1]$
- MM2: low $v_{\infty,L}$ and short ToF; $\mathbf{w}=[0.75, 1, 0]$
- MM3: low $v_{\infty,L}$ and low $v_{\infty,A}$; $\mathbf{w}=[0, 1, 1]$

In each flyby sequence, among all the trajectories found with the same strategy, similar geometry but slightly different launch date or $v_{\infty,L}$, only the one that minimises the selected MM is saved. Considering MM1 as measure of merit, Table 7 and Table 8 show the total amount of different strategies found in the global search, grouping them with respect to $v_{\infty,L}$, ToF or $v_{\infty,A}$, for each different launch year.

		Launch year				
		2007	**2008**	**2009**	**2010**	**2011**
$v_{\infty,L}$ [km/s]	$v_{\infty,L} < 3$	0	0	0	0	0
	$3 \le v_{\infty,L} < 4$	2	1	3	3	2
	$4 \le v_{\infty,L} < 5$	10	5	6	8	10
	$5 \le v_{\infty,L} < 6$	9	5	6	14	4
	$v_{\infty,L} \ge 6$	14	10	10	14	16
ToF [years]	*ToF* < 5	1	1	1	0	1
	5 ≤ *ToF* < 5.5	2	0	3	2	2
	5.5 ≤ *ToF* < 6	2	1	5	3	3
	6 ≤ *ToF* < 6.5	8	7	7	8	8
	ToF ≥ 6.5	22	12	9	26	18
$v_{\infty,A}$ [km/s]	$v_{\infty,A} < 6$	1	2	1	2	1
	$6 \le v_{\infty,A} < 7$	14	5	6	11	6
	$7 \le v_{\infty,A} < 8$	4	3	5	6	3
	$8 \le v_{\infty,A} < 9$	7	4	5	4	9
	$v_{\infty,A} \ge 9$	9	7	8	16	13

Table 7: Missions to Jupiter; Launch possibilities in the GA-only case

		Launch year				
		2007	**2008**	**2009**	**2010**	**2011**
$v_{\infty,L}$ [km/s]	$v_{\infty,L} < 3$	0	0	0	0	0
	$3 \le v_{\infty,L} < 4$	6	4	1	3	5
	$4 \le v_{\infty,L} < 5$	20	15	14	15	17
	$5 \le v_{\infty,L} < 6$	27	27	18	33	18
	$v_{\infty,L} \ge 6$	44	27	38	47	44
ToF [years]	*ToF* < 5	20	14	13	16	10
	5 ≤ *ToF* < 5.5	12	5	3	9	7
	5.5 ≤ *ToF* < 6	16	7	10	16	4
	6 ≤ *ToF* < 6.5	14	15	17	16	25
	ToF ≥ 6.5	35	32	28	41	38
$v_{\infty,A}$ [km/s]	$v_{\infty,A} < 6$	13	13	12	20	14
	$6 \le v_{\infty,A} < 7$	25	24	14	19	18
	$7 \le v_{\infty,A} < 8$	10	12	20	16	16
	$8 \le v_{\infty,A} < 9$	19	7	7	24	19
	$v_{\infty,A} \ge 9$	30	17	18	19	17

Table 8: Missions to Jupiter; Launch possibilities in the AGA+GA case($E^*=3.7$)

It is evident that the use of AGA manoeuvres in combination with or in substitution to GA allows more launch possibilities.

We analyse all solutions found and, for each different flyby sequence, we select the one that minimises the measures of merit previously defined, for both GA-only and AGA+GA strategies. The three best interplanetary paths are shown in Table 9 and in Table 10.

GA-only Flybys sequence	Launch dd	mm	yyyy	$v_{\infty,L}$ km/s	ToF s.y	$v_{\infty,A}$ km/s	MM
MM1: Low $v_{\infty,L}$, short ToF and low $v_{\infty,A}$							
V_{GA} E_{GA} E_{GA}	4	3	2009	3.75	5.66	6.28	7.76
V_{GA} E_{GA}	14	8	2011	4.00	5.87	5.98	7.88
V_{GA} M_{GA} E_{GA}	14	1	2009	4.00	5.50	7.45	8.08
MM2: Low $v_{\infty,L}$ and short ToF							
V_{GA} E_{GA} E_{GA}	1	1	2009	3.00	5.33	8.78	6.29
V_{GA} V_{GA} E_{GA}	28	1	2009	4.25	5.07	10.80	6.55
V_{GA} M_{GA} E_{GA}	14	1	2009	4.00	5.50	7.45	6.68
MM3: Low $v_{\infty,L}$ and low $v_{\infty,A}$							
V_{GA} E_{GA} E_{GA}	9	1	2007	3.50	6.85	6.21	4.84
V_{GA} V_{GA} E_{GA}	5	6	2010	3.75	6.73	6.14	4.90
V_{GA} E_{GA}	14	8	2011	4.00	5.87	5.98	4.94

Table 9: Missions to Jupiter; Best trajectories in the GA-only case

AGA+GA Flybys sequence	Launch dd	mm	yyyy	$v_{\infty,L}$ km/s	ToF s.y	$v_{\infty,A}$ km/s	MM
MM1: Low $v_{\infty,L}$, short ToF and low $v_{\infty,A}$							
V_{AGA} M_{AGA}	23	5	2007	4.25	3.81	5.12	6.74
V_{GA} E_{AGA}	30	6	2007	3.25	4.24	6.02	6.83
V_{GA} M_{AGA}	4	2	2009	4.00	3.75	6.95	7.07
MM2: Low $v_{\infty,L}$ and short ToF							
V_{AGA} M_{AGA}	19	2	2009	4.00	3.50	8.58	5.68
V_{AGA} E_{AGA}	25	9	2010	3.50	3.83	7.44	5.68
V_{GA} E_{AGA}	10	10	2010	4.00	3.69	7.91	5.78
MM3: Low $v_{\infty,L}$ and low $v_{\infty,A}$							
V_{GA} M_{AGA}	2	3	2007	4.00	6.60	4.39	4.61
V_{GA} E_{AGA}	13	9	2010	3.25	4.30	5.90	4.69
V_{AGA} M_{AGA}	30	6	2011	3.75	6.16	5.50	4.75

Table 10: Missions to Jupiter; Best trajectories in the AGA+GA case ($E^*=3.7$)

Analysing the results shown in these tables, it can be seen that in all cases the AGA+GA strategy provides better performances and better minimisation of the MMs, often with the advantage of one less planetary manoeuvre.

Furthermore, AGA often results in faster trajectories: with AGA, it is possible to obtain extremely fast missions (with ToF lower than four sidereal years) especially in case of double-AGA strategies, otherwise impossible using the GA-only strategy.

The best strategy in the GA-only case is the well-known V_{GA} E_{GA} E_{GA} (see Figure 10), that was used in the Galileo mission[5]. As it was also shown in a previous paper[7], this can provide extremely good performances, with the advantage of many launch opportunities.

In the AGA+GA case, the best trajectory (from the point of view of the more general measure of merit, that is MM1) is V_{AGA} M_{AGA} (see Figure 11).

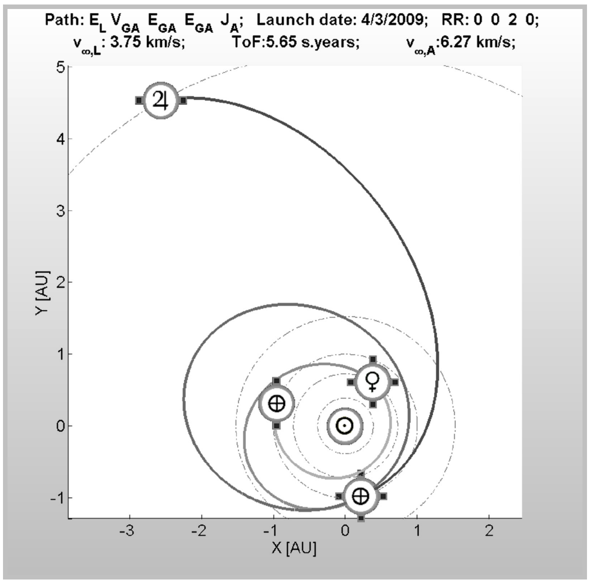

Figure 10: Missions to Jupiter; GA-only case; trajectory that minimise MM1

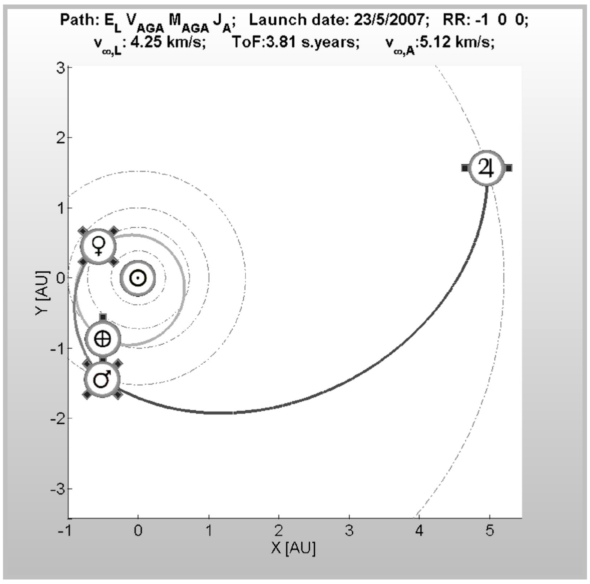

Figure 11: Missions to Jupiter; AGA+GA case; trajectory that minimise MM1

If a short ToF isn't a primary target, the V_{GA} M_{AGA} and the V_{GA} E_{AGA} strategies can provide interesting performances. Furthermore, these make use of only one aerogravity assist manoeuvre; this fact is advisable with respect to multiple AGA trajectories, due to the high ablation of materials during the atmospheric passages.

<u>Phasing feasibility study: Missions to Neptune</u>

Neptune is a target that still needs to be better investigated. In fact, only the Voyager 2 mission observed it from a short distance, during a flyby. A Neptune orbiter could provide a greater amount of scientific observations. A mission to Neptune is highly demanding, because of its high distance from the Sun (in certain periods, when Pluto is near to the periapsis of its eccentric orbit, Neptune is the most distant planet from the Sun).

We study the interplanetary transfer for this mission, using again our software for an automated trajectory search with phasing considerations. We consider a time period of 15 years, from the 1st of January 2005 to the 1st of January 2020, assuming a maximum $v_{\infty,L}$ of 9 km/s and a maximum ToF for the interplanetary transfer equal to 15 sidereal years. We consider an increased value of the maximum aerodynamic efficiency ($E^*=5$); this value is feasible for future missions, considering the current developments in the field of waveriders design[12].

All the others parameters are set equal to those previously used for missions to Jupiter. On the basis of a previous energy-based study, we analyse 36 different flyby sequences for GA-only and 37 for AGA+GA. Also this time, due to bad planetary phasing, some paths feasible after the A-type study give no real results for the considered time span; confirming the previous considerations about increased launch opportunities using AGA manoeuvres, in the GA-only case 8 paths resulted feasible, while in AGA+GA case only 3 paths gave no results.

Due to the far distance of the final target, in the definition of the various MMs (see (10)) we still gave the same weights to ΔVs for Earth escape and for final orbit insertion, but we give a greater importance to the ToF with respect to fuel consumption:

- MM1: low $v_{\infty,L}$ and $v_{\infty,A}$, short ToF; **w**=[1.5, 1, 1]
- MM2: low $v_{\infty,L}$ and short ToF; **w**=[1.5, 1, 0]
- MM3: low $v_{\infty,L}$ and low $v_{\infty,A}$; **w**=[0, 1, 1]

We group the results as for missions to Jupiter. These are shown in Table 11 and Table 12.

As it can be seen from the tables, AGA+GA strategy confirms its overall better performances with respect to missions using only gravity assist. Due to the high-energy requirements of this mission, in the GA-only case it is possible to reach Neptune only with one or two flybys of giant planets, thus considerably limiting launch windows. Furthermore, ToF remains always high.

With AGA, it is possible to reach the final target also with only two swingbys of internal planets (M_{AGA} V_{AGA}, V_{AGA} E_{AGA}, V_{AGA} M_{AGA}). The flyby sequence M_{AGA} V_{AGA}, not previously considered in similar studies[8,9], gives promising results, being the best from MM1 point of view. With AGAs it is also possible to complete the interplanetary transfer in less than 7 sidereal years. If ToF is not considered in trade-offs, the strategy V_{GA} E_{GA} M_{AGA} allows extremely low fuel consumption for the Earth-escape and Neptune-insertion ΔVs.

GA-only Flybys sequence	**Launch** dd	mm	yyyy	**$v_{\infty,L}$** km/s	**ToF** s.y	**$v_{\infty,A}$** km/s	**MM**
MM1: Low $v_{\infty,L}$, short ToF and low $v_{\infty,A}$							
M_{GA} E_{GA} J_{GA}	30	3	2016	6.25	12.06	14.21	28.28
J_{GA} S_{GA}	18	12	2016	9.00	12.67	12.83	29.88
V_{GA} E_{GA} E_{GA} J_{GA}	1	5	2015	4.75	14.47	12.51	30.16
MM2: Low $v_{\infty,L}$ and short ToF							
M_{GA} E_{GA} J_{GA}	13	3	2016	6.50	11.98	14.43	22.96
V_{GA} E_{GA} E_{GA} J_{GA}	31	8	2013	4.75	13.00	19.66	23.71
J_{GA} S_{GA}	18	12	2016	9.00	12.67	12.83	25.44
MM3: Low $v_{\infty,L}$ and low $v_{\infty,A}$							
M_{GA} E_{GA} J_{GA}	29	2	2016	7.00	14.81	10.29	8.25
V_{GA} E_{GA} E_{GA} J_{GA}	1	5	2015	4.75	14.47	12.51	8.46
V_{GA} V_{GA} E_{GA} J_{GA}	10	7	2015	6.50	14.81	12.28	9.11

Table 11: Missions to Neptune; Best trajectories in the GA-only case

AGA+GA Flybys sequence	**Launch** dd	mm	yyyy	**$v_{\infty,L}$** km/s	**ToF** s.y	**$v_{\infty,A}$** km/s	**MM**
MM1: Low $v_{\infty,L}$, short ToF and low $v_{\infty,A}$							
M_{AGA} V_{AGA}	8	11	2009	7.00	8.68	15.47	24.44
V_{AGA} M_{AGA}	20	4	2006	7.25	9.07	14.52	24.51
M_{AGA} V_{AGA} J_{GA}	2	9	2007	7.25	9.44	14.52	25.08
MM2: Low $v_{\infty,L}$ and short ToF							
V_{AGA} E_{AGA} J_{GA}	5	1	2019	9.00	6.38	28.25	16.01
M_{AGA} V_{AGA}	9	11	2009	7.25	7.33	19.22	16.39
V_{AGA} E_{AGA}	26	5	2019	8.75	7.07	21.54	16.88
MM3: Low $v_{\infty,L}$ and low $v_{\infty,A}$							
V_{GA} E_{GA} M_{AGA}	14	11	2011	3.25	14.36	9.61	6.34
V_{AGA} V_{GA} E_{AGA}	4	2	2009	4.75	14.93	8.75	6.43
V_{AGA} M_{AGA}	15	10	2013	6.00	14.85	7.54	6.45

Table 12: Missions to Neptune; Best trajectories in the AGA+GA case

CONCLUSIONS

In this paper an extensive analysis of several transfer trajectories either to the Sun or to outer planets has been presented, comparing performances offered by aerogravity assist manoeuvres with respect to simple gravity assist ones.

To this aim, a specific software tool, named PAMSIT, was developed to help mission analysts in preliminary design of multiple swingbys trajectories with GA and AGA manoeuvres.

The technique used in PAMSIT is a systematic global search based on some simplifying assumptions on the physical model of the Solar System. The results, obtained in a very short computational time, were accurate, demonstrating that the method is effective for both preliminary mission design and for first guess generation.

A first analysis was performed with an energy-based method, without taking into account the real position

of the planets, showing how AGA can allow faster missions than simple GA at comparable ΔV-cost. Furthermore, AGA resulted to be more flexible, allowing more frequent launch opportunities compared to the GA-only ones, due the higher dependency of the latter on the phasing of planets.
This was demonstrated in a second analysis, in which the phasing of the planet was included in a slightly improved model. In particular, missions to Jupiter and to Neptune were considered as an example, giving an exhaustive comparison between the two different strategies. The advantages of AGA were confirmed, showing how it improves the performances considering both the TOF of the entire mission and the propellant consumption necessary to perform the escape from Earth and the insertion in the final orbit around the target planet.
Other issues will be investigated in future works introducing constraints in the dynamic model, like aerodynamic heating, ablation of materials during the atmospheric flight, dependence of performances on aerodynamic shape of the spacecraft and on AGA parameters.

ACKNOWLEDGEMENTS

We are particularly grateful to Eugene Bonfiglio and James M. Longuski for their support in the comprehension of the AGA dynamics.

REFERENCES

1: Randolph J. E., McRonald A. D., “Solar Probe Mission Status”, American Astronautical Society, Paper 89-212, April 1989.
2: McRonald A. D., Randolph J. E., “Hypersonic Maneuvering for Augmenting Planetary Gravity Assist”, Journal of Spacecraft and Rockets, Vol.39, No.2, March-April 1992, pp.216-222.
3: McRonald A. D., Randolph J. E., “Solar System ‘Fast Mission’ Trajectories Using Aerogravity Assist”, Journal of Spacecraft and Rockets, Vol.39, No.2, March-April 1992, pp.223-232.
4: Lohar F.A., Misra A.K., Mateescu D. , “Mars-Jupiter Aerogravity assist trajectories for high energy missions”, Journal of Spacecraft and Rockets, Vol.34, No.1, 1997.
5: Rinderle, E, A., “Galileo User’s Guide, Mission Design System, Satellite Tour Analysis and Design Subsystem”, Jet Propulsion Laboratory, Rept. JPL D-263, California Institute of Technology, Pasadena, CA, July 1986.
6: Williams S. N., “Automated Design of Multiple Encounter Gravity-Assist Trajectories”, Master Thesis, Purdue University, August 1990.
7: Petropoulos, A. E., Longuski, J. M, and Bonfiglio, E. P., "Trajectories to Jupiter via Gravity Assists from Venus, Earth, and Mars," Journal of Spacecraft and Rockets, Vol. 37, No. 6, 2000, pp. 776-783.
8: Bonfiglio E., “Automated Design of Gravity-Assist and Aerogravity-Assist Trajectories”, Master of Science Thesis, School of Aeronautics and Astronautics, Purdue Univ., West Lafayette, IN, August 1999.
9: Bonfiglio E., Longuski J.M., Vinh N.X., “Automated Design of Aerogravity-Assist Trajectories”, Journal of Spacecraft and Rockets, Vol.37, No.6, November-December 2000, pp.768-776.
10: Strange J. S., Longuski J. M., “Graphical Method for Gravity-Assist Trajectory Design”, Journal of Spacecraft and Rockets, Vol.39, No.1, January-February 2002, pp.9-16.
11: Johnson W. R. and Longuski J. M., “Design of Aerogravity Trajectories”, Journal of Spacecraft and Rockets, Vol.39, No.1, January-February 2002, pp.23-30.
12: McRonald A. D., Randolph J. E., Lewis M. J., Bonfiglio E. P., Longuski J., Kolodziej P., “From LEO to Planets Using Waveriders”, AIAA 99-4803.
13: Yen C. L., “Ballistic Mercury Orbiter Mission via Venus and Mercury Gravity Assists”, The Journal of the Astronautical Sciences, Vol.37, No.3, July-September 1989, pp.417-432.
14: Vasile M., “Direct Transcription by FET for Optimal Space Trajectory Design”, Internal Report DIA-SR 99-02, Dip. di Ingegneria Aerospaziale, ‘Politecnico di Milano’ university, Milan, Italy, March 1999.
15: Vasile M., Bernelli-Zazzera F., “Combining Low-Thrust Propulsion and Gravity Assist Manoeuvres to Reach Planet Mercury”, AAS 01-459, AAS/AIAA Astrodynamics Specialist Conference, Quebec City, Quebec, Canada, July 30-August 2, 2001.
16: Campagnola S., “Missioni su Europa: Traiettorie Ottime mediante Propulsione Elettrica Ausiliaria e Flyby Gravitazionali”, Master Thesis, Dipartimento di Ingegneria Aerospaziale, ‘Politecnico di Milano’ university, Milan, Italy, June 2002.
17: Campagnola S., Vasile M., Bernelli-Zazzera F. “Electric Propulsion Options for a Probe to Europa”, Lotus 2 – Second Low Thrust International Symposium, CNES, IAS, Toulouse, France, 18-20 June, 2002.
18: Vasile M., Biesbroek R., Summerer L., Galvez A., Kminek G., “Options for a Mission to Pluto and Beyond”, Paper AAS 03-210, 13th AAS/AIAA Space Flight Mechanics Meeting, Ponce, Puerto Rico, 9-13 February 2003.
19: Pessina S. M., “Analisi Preliminare di Traiettorie Interplanetarie con Manovre Aerogravitazionali”, Master Thesis, Dipartimento di Ingegneria Aerospaziale, ‘Politecnico di Milano’ university, Milan, Italy, February 2003.
20: Lewis M. J., McRonald A. D., “Design of Hypersonic Waveriders for Aeroassisted Interplanetary Trajectories”, Journal of Spacecraft and Rockets, Vol.29, No.5, September-October 1992, pp.653-662.
21: Colin, Donahue, and Moroz, “Data from Venus”, Appendix A, 1046-1048, Hunten, U, Arizona, 1983.
22: “MSIS-E-90 Model”, NASA, National Space Science Data Center. *http://nssdc.gsfc.nasa.gov/space/model/models/msis.html*
23: “Mars Pathfinder Atmospheric Structure Instrument / Meteorology Package”, NASA, Planetary Data System. *http://atmos.nmsu.edu/PDS/data/mpam_0001*
24: Gillum M. J., Lewis M. J., “Experimental Results on a Mach 14 Waverider with Blunt Leading Edges”, Journal of Spacecraft and Rockets, Vol.34, No.3, May-June 1997, pp.296-303.